PHYSICAL REVIEW B VOLUME 34, NUMBER 11 1 DECEMBER 1986

Magnetic susceptibility of $MnCl_2$- and $CoCl_2$-graphite intercalation compounds

D. G. Wiesler, M. Suzuki,* P. C. Chow, and H. Zabel

Department of Physics and Materials Research Laboratory, University of Illinois at Urbana-Champaign,
1110 West Green Street, Urbana, Illinois 61801

(Received 31 July 1986)

The dc magnetic susceptibilities of $MnCl_2$-graphite intercalation compounds (GIC's) (stages 1 and 2) and $CoCl_2$-GIC's (stages 1, 2, and 3) were measured between 2 and 300 K for external field orientations both perpendicular and parallel to the c axis. $MnCl_2$-GIC obeys a Curie-Weiss law for both orientations above 20 K, with g factors close to the spin-only value of 2.0 for both stages. The measured Curie-Weiss temperatures indicate a net antiferromagnetic intraplanar exchange interaction, with a small XY anisotropy appearing below about 50 K. $CoCl_2$-GIC, in contrast, exhibits considerable XY anisotropy at all temperatures. The susceptibility perpendicular to the C axis has been fit to a Curie-Weiss law above 120 K, yielding a stage-dependent ferromagnetic intraplanar exchange ($J=10.4$, 7.7, and 6.8 K for stages 1, 2, and 3, respectively). The susceptibility parallel to the c axis contains a very large temperature-independent term which can be attributed to Van Vleck paramagnetism.

I. INTRODUCTION

In a stage-N transition-metal-chloride—graphite intercalation compound (GIC), magnetic MCl_2 layers ($M=$Co or Mn) are separated periodically by N graphite layers in stacks along the c axis. The interplanar interaction between adjacent magnetic layers can be systematically reduced by increasing the stage number N, while the intraplanar exchange remains virtually unchanged. The intercalate layers of both $CoCl_2$- and $MnCl_2$-GIC's form a planar triangular lattice, nearly identical to the pristine compounds. The intercalation compounds, therefore, provide an excellent system for studying magnetic phase transitions on triangular lattice sites.

The magnetic properties of $MnCl_2$-GIC's have been investigated by several authors.[1-5] Both the stage-1 and -2 compounds have shown a magnetic phase transition at $T_c=1.2$ K. Recent neutron scattering studies[5] below T_c suggest an in-plane spin structure with a $(2\sqrt{3}\times2\sqrt{3})$ periodicity having spins lying in the intercalate plane, while the high-temperature phase is paramagnetic. An anomaly in the specific heat at 50 K (Ref. 1) was originally thought to be an upper-phase transition. However, no additional evidence has been accumulated for this interpretation.

The magnetic properties of $CoCl_2$-GIC's have been studied in great detail by a variety of experimental probes.[5-11] Neutron scattering studies[10] have revealed a two-step magnetic ordering process. Above $T_u=9.1$ K the compounds are paramagnetic. Below this temperature the compounds order ferromagnetically within the intercalate planes, but with no correlation between different planes. Below $T_l=8.0$ K the ferromagnetic sheets become weakly antiferromagnetically correlated along the c axis.

In this paper we report experimental results on the magnetic susceptibility of stage-1 and -2 $MnCl_2$-GIC's and stage-1, -2, and -3 $CoCl_2$-GIC's based on single crystals of Kish graphite. We shall analyze the data using model effective spin Hamiltonians presented in Sec. III and determine from experimental data their parameters.

II. CRYSTAL STRUCTURE

The intercalate layer of MCl_2 consists of a three-layer sandwich of Cl-M-Cl layers, with the same layered structure as pristine MCl_2. The distance between adjacent graphite layers increases from 3.35 to 9.30 Å (Ref. 7) upon intercalation, giving repeat distances of roughly 9.30, 12.65, and 16.00 Å for stages 1, 2, and 3, respectively.

The intercalate layers form triangular lattices translationally incommensurate with the graphite host but rotationally locked into 30° with respect to it.[7] Intercalation changes the in-plane lattice parameters only slightly from their pristine values [3.67 Å in $MnCl_2$-GIC (Ref. 12) and 3.54 Å in $CoCl_2$-GIC (Ref. 7)]. The intercalate layer consists of small islands whose size is estimated as 130 Å in $MnCl_2$-GIC,[12] and 420 Å in $CoCl_2$-GIC.[10,11]

III. THEORY

A. $MnCl_2$-GIC

Since a Mn^{2+} ion has no orbital angular momentum in the free-ion $3d^5\,{}^6S$ state, its sixfold spin degeneracy is split only by the higher-order perturbation of the spin-orbit interactions through intermediate excited states. The Hamiltonian appropriate to Mn^{2+} ions in this compound may be written as [13]

$$\mathscr{H}=2J\sum_{i,j}\mathbf{S}_i\cdot\mathbf{S}_j+D\sum_i(S_i^z)^2+2J'\sum_{i,m}\mathbf{S}_i\cdot\mathbf{S}_m\ , \tag{1}$$

where J is the antiferromagnetic intraplanar exchange interaction, J' is the much weaker interplanar exchange, and D is the single-ion anisotropy parameter.

If D is nonzero then the susceptibilities measured with

©1986 The American Physical Society

external field **H**⊥**c** and **H**||**c** will be different. At high temperatures they take the form[13]

$$\chi_i=\frac{C_i}{T+\Theta_i}\quad (i=||,\perp)\ , \tag{2}$$

with $\Theta_{||}=\Theta+2P$ and $\Theta_\perp=\Theta-P$, where P relates to the anisotropy constant by the relation

$$P=D[\tfrac{2}{15}S(S+1)-\tfrac{1}{10}]\ . \tag{3}$$

C_i and Θ are the usual Curie constants and Curie-Weiss temperature given by

$$C_i=\frac{N_A g_i^2\mu_B^2 S(S+1)}{3k_B}\ , \tag{4}$$

$$\Theta=\tfrac{2}{3}zJS(S+1)\ , \tag{5}$$

for coordination number $z=6$, spin $S=\frac{5}{2}$, and Avogadro number N_A. At 0 K the susceptibility can be obtained from molecular field theory as[13]

$$\chi_\perp(0)=\frac{N_A g_\perp^2\mu_B^2}{4k_B zJ}\ . \tag{6}$$

B. CoCl$_2$-GIC

The Hamiltonian appropriate to Co^{2+} ions in this compound is assumed to be of similar form to that of pristine CoCl$_2$, discussed in detail by Lines.[14] The combined effect of spin-orbit coupling and trigonal distortion of the crystal field splits the ground-state orbital triplet $^4T_1$ into six Kramers doublets. This perturbing Hamiltonian may be written as

$$\mathscr{H}_0=-\tfrac{3}{2}k\lambda\mathbf{l}\cdot\mathbf{S}-\delta(l_z^2-\tfrac{2}{3})\ , \tag{7}$$

where λ is the spin-orbit coupling constant, **S** is the spin angular momentum of magnitude $\frac{3}{2}$, **l** is a fictitious orbital momentum of magnitude 1, δ is the trigonal field strength, and k is the orbital reduction factor due to admixture of ^4P into $^4T_1$. Following Lines,[14] we take $k=0.9$ and define $\lambda'=k\lambda$.

Since l_z+S_z is a constant of motion, its eigenvalue m can be used to classify various states. We use the notation $|l_z,S_z\rangle$ to specify 12 states. The secular equation reduces to three separate equations for the energy eigenvalues: one linear $E_{\pm6}=E_l$ $(m=\pm\frac{5}{2})$; one quadratic $E_{\pm2}=E_q^{(+)}$, $E_{\pm5}=E_q^{(-)}$ $(m=\pm\frac{3}{2})$; and one cubic $E_{\pm1}=E_c^{(0)}$, $E_{\pm3}=E_c^{(1)}$, $E_{\pm4}=E_c^{(2)}$ $(m=\pm\frac{1}{2})$. For $\delta/\lambda'>0$, $E_{\pm1}<E_{\pm2}<\cdots<E_{\pm6}$. The ground-state wave function is given by

$$|\psi_{\pm1}\rangle=c_1|\mp1,\pm\tfrac{3}{2}\rangle+c_2|0,\pm\tfrac{1}{2}\rangle+c_3|\pm1,\mp\tfrac{1}{2}\rangle\ , \tag{8}$$

where the coefficients c_i are determined via a parameter ξ defined by[14,15]

$$E_{\pm1}=-\tfrac{1}{3}\delta+\tfrac{3}{4}\lambda'(\xi+3)\ . \tag{9}$$

It is straightforward to show that

$$\frac{\delta}{\lambda'}=\tfrac{3}{4}(\xi+3)-\frac{9}{2\xi}-\frac{6}{\xi+2}\ , \tag{10}$$

$$c_1:c_2:c_3=\sqrt{6}/\xi:-1:\sqrt{8}/(\xi+2)\ . \tag{11}$$

In an external field H, the energy splitting of the lowest Kramers doublet by the perturbation

$$\mathscr{H}'=\mu_B H^z V_{||}\quad (V_{||}=-\tfrac{3}{2}kl_z+2S_z)\ , \tag{12}$$

can be written as $sg_{||}^{(1)}\mu_B H^z$, where s is a fictitious spin of magnitude $\frac{1}{2}$ and

$$\begin{aligned} g_{||}^{(1)}&=2\langle\psi_{\pm1}|V_{||}|\psi_{\pm1}\rangle\\ &=\frac{6(6+3k)/\xi^2+2-8(2+3k)/(\xi+2)^2}{6\xi^{-2}+1+8/(\xi+2)^2}\ . \end{aligned} \tag{13}$$

Similarly, we may define $g_\perp^{(1)}$ as

$$\begin{aligned} g_\perp^{(1)}&=2\langle\psi_{\pm1}|V_\perp|\psi_{\pm1}\rangle\\ &=\frac{4[1+12/\xi(\xi+2)+3k/(\xi+2)]}{6\xi^{-2}+1+8/(\xi+2)^2}\ , \end{aligned} \tag{14}$$

where $V_\perp=-\frac{3}{2}kl_x+2S_x$. When small admixing of the upper orbital triplet $^4T_2$ into the ground orbital triplet $^4T_1$ is taken into account, the resultant g values are[14]

$$\begin{aligned} g_{||}&=g_{||}^{(1)}+\Delta g\ ,\\ g_\perp&=g_\perp^{(1)}+\Delta g\ , \end{aligned} \tag{15}$$

where $\Delta g_\perp=\Delta g_{||}=\Delta g$ is assumed. Once the values of $g_\perp$ and $g_{||}$ are determined experimentally, the values of $g_\perp^{(1)}$, $g_{||}^{(1)}$, ξ, and δ/λ' can be obtained uniquely using Eqs. (13) and (14) and the relation $g_\perp-g_{||}=g_\perp^{(1)}-g_{||}^{(1)}$.

The spin Hamiltonian of CoCl$_2$-GIC can be expressed using the fictitious spin **s** of magnitude $\frac{1}{2}$ by[14]

$$\mathscr{H}=-2J\sum_{i,j}\mathbf{s}_i\cdot\mathbf{s}_j+2J_A\sum_{i,j}s_i^zs_j^z+2J'\sum_{i,m}\mathbf{s}_i\cdot\mathbf{s}_m\ , \tag{16}$$

where J_A is the anisotropic exchange interaction, given by

$$\frac{J_A}{J}=1-\left[\frac{1+18(\xi+2)^{-1}-8(\xi+2)^{-2}}{2+24/\xi(\xi+2)}\right]^2\ . \tag{17}$$

For $\xi>2$, J_A/J is positive and the spin system is XY-like.

At temperatures much higher than T_l, χ_i may be described by

$$\chi_i=\chi_i^{VV}+\frac{C_i}{T-\Theta_i}\quad (i=\perp,||)\ , \tag{18}$$

with $\Theta_\perp=\Theta$ and C_i given by Eqs. (4) and (5) for the case $s=\frac{1}{2}$. χ_i^{VV} is the Van Vleck temperature-independent susceptibility given by[14]

$$\chi_i^{VV}=2N_A\mu_B^2\sum_{n=2}^{6}\frac{|\langle\psi_n|V_i|\psi_{\pm1}\rangle|^2}{E_n-E_1}\ . \tag{19}$$

The susceptibility at 0 K can be obtained from molecular-field theory as[14]

$$\chi_\perp(0)=\frac{N_A g_\perp^2\mu_B^2}{4k_B z'J'}\ , \tag{20}$$

where z' is the interplanar coordination number, 6.

IV. EXPERIMENTAL PROCEDURE

The samples of $MnCl_2$- and $CoCl_2$-GIC's were prepared from single-crystal Kish graphite by vapor reaction of the powdered metal chloride in a chlorine gas atmosphere of 740 torr. Staging of the compounds was checked by x-ray diffraction using Mo $K\alpha$ radiation. Each sample measured approximately $4\times3\times0.4\,\mathrm{mm}^3$.

Weight uptake measurements after intercalation give the following chemical compositions: $C_{8.8}MnCl_{2.4}$ and $C_{12.3}MnCl_{2.4}$ for stage-1 and -2 $MnCl_2$-GIC's; $C_{5.0}CoCl_{2.03}$, $C_{10.6}CoCl_{2.03}$, and $C_{14.7}CoCl_{2.03}$ for stage-1, -2, and -3 $CoCl_2$-GIC's, respectively. The excess of chlorine can be attributed to incompleteness of the intercalate layers due to island formation. In the formulas above the [Mn]/[Cl] ratio is taken from Baron *et al.*,[12] while the [Co]/[Cl] ratio is based on charge transfer considerations with 420-Å intercalate islands.[10,11]

Magnetic susceptibility measurements were made using a SHE VT-50 superconducting quantum-interference device (SQUID) susceptometer at temperatures between 2.0 and 300 K and for fields up to 40 kOe.

V. RESULTS AND ANALYSIS

A. $MnCl_2$-GIC

Figure 1 shows the magnetizations $M_{\parallel}$ and $M_{\perp}$ of the stage-2 compound as a function of external field at various temperatures. M is linear in H for fields up to 40 kOe at temperatures above 20 K. A field of 1 kOe was thus chosen for all measurements. Susceptibilities have been corrected for core diamagnetism χ_d using the following values: $\chi_c=-6\times10^{-6}$, $\chi_{\mathrm{Mn}}=-14\times10^{-6}$, and $\chi_{\mathrm{Cl}}=-20.1\times10^{-6}$ (all in emu/ mol). χ_d is estimated to be -1.15×10^{-4} emu/mol of spins for the stage-1 compound and -1.36×10^{-4} emu/mol for the stage-2 compound.

Figure 2(a) shows the temperature dependence of $\chi_{\parallel}$ and $\chi_{\perp}$ in the stage-2 compound. Both $\chi_{\parallel}$ and $\chi_{\perp}$ decrease monotonically with increasing temperature and exhibit no anomaly around 50 K, where the magnetic specific heat shows a broad peak.[1] $\chi_{\perp}>\chi_{\parallel}$ at all temperatures, which suggests that spins align in the intercalate plane. The anisotropy $\Delta\chi=\chi_{\perp}-\chi_{\parallel}$ becomes appreciable only below 50

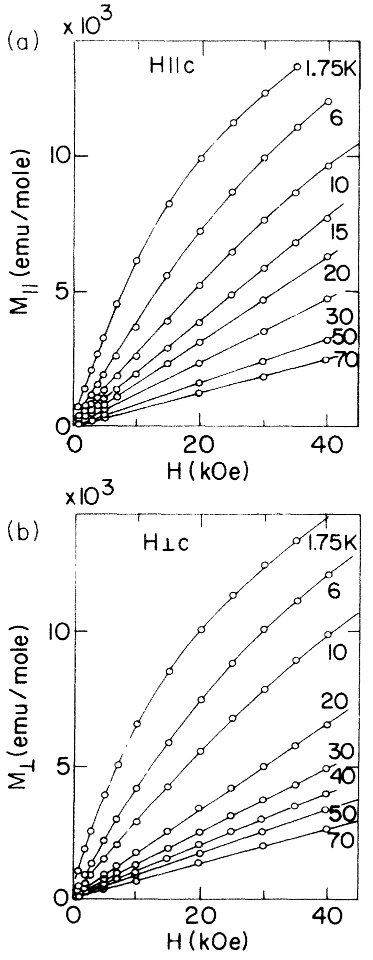

FIG. 1. A series of field dependence measurements at various temperatures in stage-2 $MnCl_2$-GIC. (a) $H\parallel c$; (b) $H\perp c$.

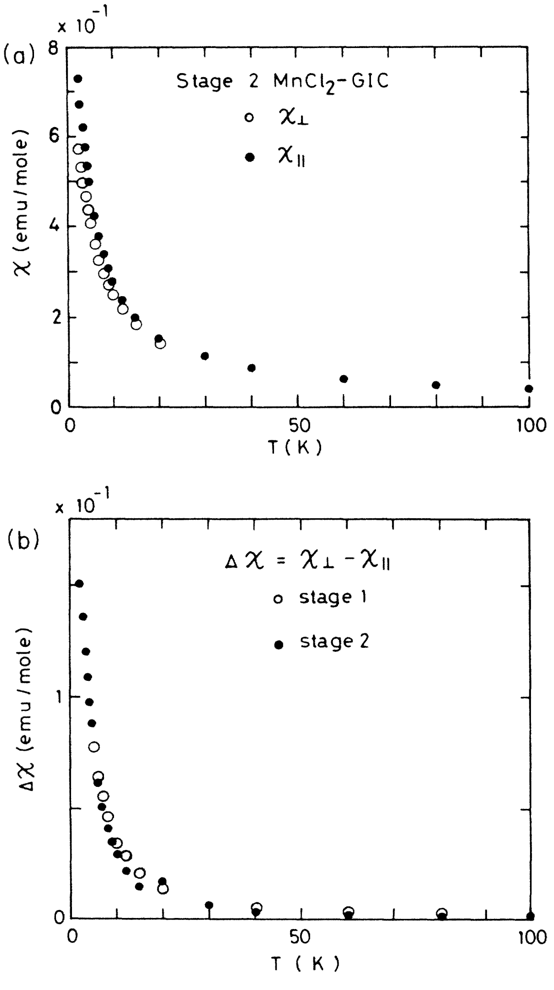

FIG. 2. (a) Temperature dependence of susceptibilities in two field directions for stage-2 $MnCl_2$-GIC; (b) anisotropy $\Delta\chi$ for stage-1 and -2 $MnCl_2$-GIC's.

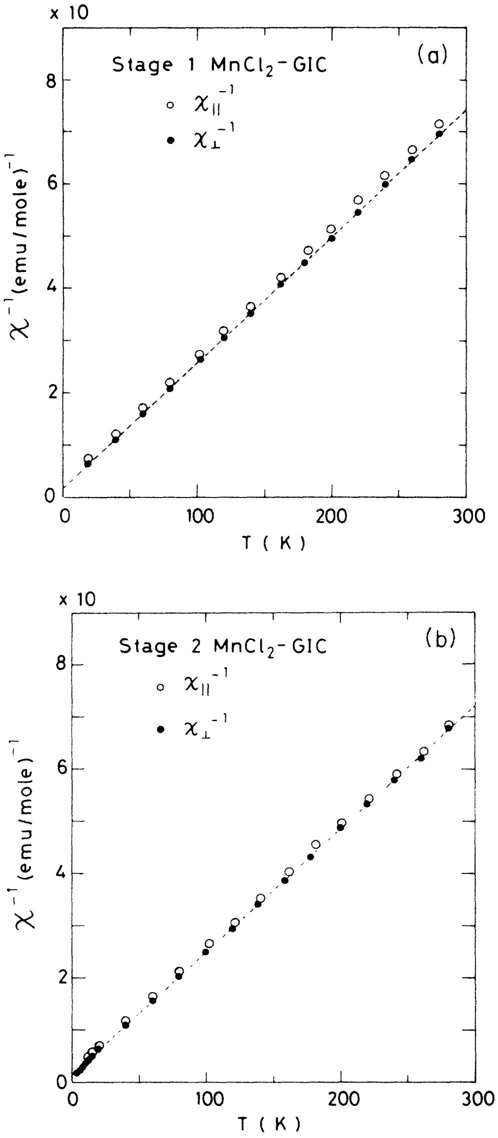

FIG. 3. Temperature dependence of reciprocal susceptibilities of MnCl$_2$-GIC's: (a) stage 1 and (b) stage 2.

K [Fig. 2(b)], a result which, along with the specific-heat anomaly and a shift of the g-values below 50 K,[1,2] may indicate the onset of short-range spin ordering in the intercalate layer.

TABLE I. Parameters of the spin Hamiltonian for stage-1 and -2 MnCl$_2$-GIC's.

	MnCl$_2$-GIC's	
	Stage 1	Stage 2
$\Theta_{\parallel}$ (K)	7.2	9.1
$\Theta_{\perp}$ (K)	5.4	5.9
$C_{\parallel}$ (emu K/mol)	4.01	4.25
$C_{\perp}$ (emu K/mol)	4.12	4.26
$g_{\parallel}$	1.91	1.97
$g_{\perp}$	1.94	1.97
J (K)	0.17	0.20
D (K)	0.56	0.97

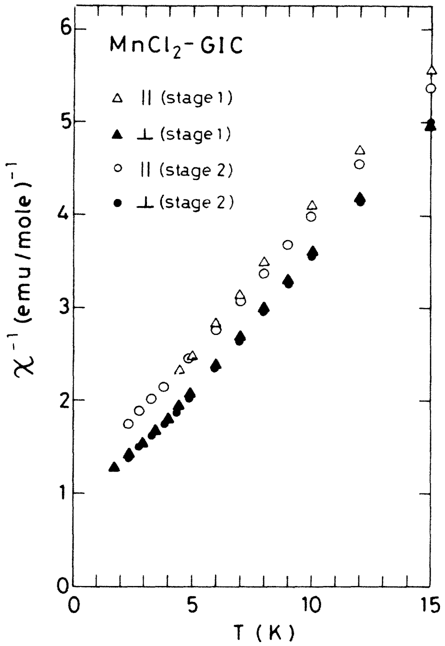

FIG. 4. Temperature variation of $\chi_{\perp}^{-1}$ and $\chi_{\parallel}^{-1}$ for stage-1 and -2 MnCl$_2$-GIC's at low temperature.

Figures 3 (a) and 3(b) show the temperature dependence of the reciprocal susceptibilities $\chi_{\parallel}^{-1}$ and $\chi_{\perp}^{-1}$ for stage-1 and -2 compounds. Both $\chi_{\parallel}$ and $\chi_{\perp}$ obey the Curie-Weiss law above 20 K. Least-squares fits of these data to Eq. (2) yield the Curie-Weiss temperatures ($\Theta_{\parallel}$,$\Theta_{\perp}$) and Curie constants ($C_{\parallel}$,$C_{\perp}$) shown in Table I. The g-factors are obtained from Eq. (4) and have values close to the spin-only value of 2.0. The parameters J and D in the spin Hamiltonian (1) are computed from $\Theta_{\parallel}$ and $\Theta_{\perp}$ and appear with $g_{\parallel}$ and $g_{\perp}$ in Table I.

Below 15 K, the susceptibilities deviate from the Curie-Weiss law (Fig. 4), due to the rapid growth of short-range spin ordering within the MnCl$_2$ layers. The value of $\chi_{\perp}$ at 0 K can be calculated by Eq. (6) to be

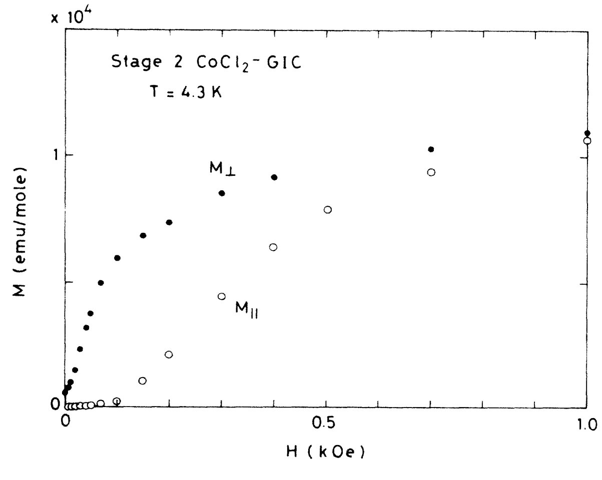

FIG. 5. Field dependence of the magnetization at 4.3 K in stage-2 CoCl$_2$-GIC with **H**⊥**c** and **H**∥**c**.

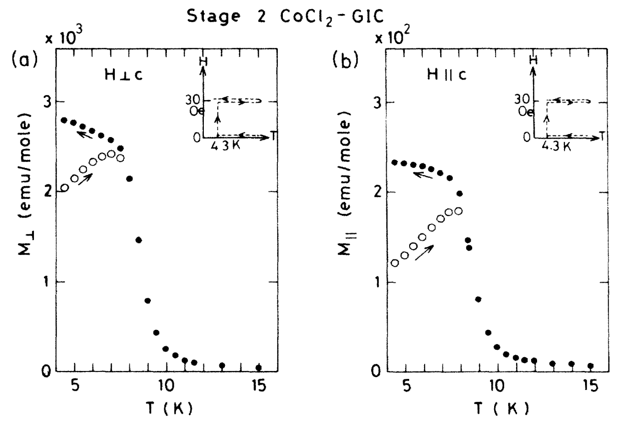

FIG. 6. Zero-field cooling measurement of the magnetization in stage-2 $CoCl_2$-GIC: (a) **H**$\perp$c and (b) **H**$\parallel$c.

$\chi_\perp(0)=0.34$ emu/mol (stage 1) and 0.30 emu/mol (stage 2). These values are smaller than the values measured above T_c at 2.0 K, a result which is consistent with an antiferromagnetic intraplanar exchange interaction and with XY spin symmetry, but is incompatible with Ising symmetry along the c axis.

B. $CoCl_2$-GIC

Figure 5 shows the field dependence of the magnetization of $CoCl_2$-GIC samples at 4.3 K with external field parallel and perpendicular to the c axis. Most striking is the strong XY anisotropy, manifested in the fact that $M_\parallel \ll M_\perp$. The sudden increase in $M_\perp$ at $H_c \sim 10$—20 Oe can be attributed to spin flopping, in which the weak interplanar antiferromagnetic alignment is broken by the stronger external field. This behavior agrees quite well with neutron scattering experiments,[7] showing H_c in the same range.

The ratio J'/J is given by Eq. (20) as

$$\frac{J'}{J}=(0.0156\ \text{emu K/mol})\frac{g_\perp^2}{J\chi_\perp(0)}\ . \qquad (21)$$

$\chi_\perp$ is strongly field dependent, but an estimate of this ratio may be made by taking the 10-Oe value of 95.6 emu/mol. As we shall show below, $J=7.75$ K and $g_\perp=6.40$, to give J'/J approximately 8.6×10^{-4}, which is consistent with the value estimated from neutron scattering measurements.

Figure 6 shows the temperature dependence of $M_\perp$ and $M_\parallel$ in the stage-2 compound, obtained as follows. The sample was first cooled at zero field to 4.3 K. Next, the field was increased to $H_0=30$ Oe. According to Fig. 5, this field is above the spin-flop field for $M_\perp$ but below the saturation field at 4.3 K. Finally, the magnetization was measured with increasing temperature to 25 K and again with decreasing temperature. There are two effects of note in this experiment. First, $M_\parallel$ and $M_\perp$ are about an order of magnitude different, which can be understood in light of the XY spin symmetry and from the fact that H_0 was chosen much below the saturation field. Second, $M_\parallel$ and $M_\perp$ show noticeable thermal hysteresis only below T_l (8.0 K), which indicates that magnetic domains exist below T_l.

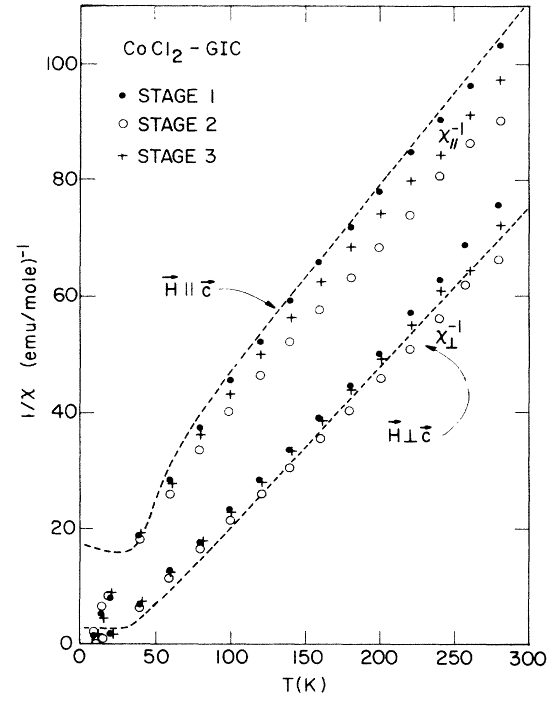

FIG. 7. Temperature dependence of reciprocal susceptibilities of $CoCl_2$-GIC's at 1 kOe for both field orientations. The dashed line refers to data for pristine $CoCl_2$ [after Bizette *et al.* (Ref. 17)].

No field dependence of χ was found above 20 K in the field range up to 40 kOe, and a field of $H=1$ kOe was chosen for the susceptibility measurements of $CoCl_2$-GIC's. $\chi_\perp$ and $\chi_\parallel$ for stage-1, -2, and -3 compounds are plotted versus temperature in Fig. 7. Least-squares fits of

TABLE II. Parameters of the spin Hamiltonian for stage-1, -2, and -3 $CoCl_2$-GIC's determined from susceptibility data with **H**$\perp$c.

		$CoCl_2$-GIC's	
	Stage 1	Stage 2	Stage 3
$\Theta_\perp$ (K)	31.1	23.2	20.3
$C_\perp$ (emu K/mol)	3.30	3.84	3.64
$\chi_\perp^0$ (emu/mol)	-0.65×10^{-4}	-0.85×10^{-4}	-1.57×10^{-4}
$g_\perp$	5.94	6.40	6.23
J (K)	10.38	7.75	6.75
χ_d (emu/mol)	-0.82×10^{-4}	-1.16×10^{-4}	-1.40×10^{-4}

the $\chi_\perp$ data above 120 K to a constant plus Curie-Weiss term,

$$\chi_\perp = \chi_\perp^0 + \frac{C_\perp}{T - \Theta_\perp} , \tag{22}$$

yield the values of $\Theta_\perp$, $C_\perp$, and $\chi_\perp^0$ shown in Table II. J and $g_\perp$ are obtained from Eqs. (4) and (5) with $s = \frac{1}{2}$ and $\Theta_\perp = \Theta$, and are also shown in Table II. Note that J decreases with increasing stage number. In pristine $CoCl_2$, J has been reported alternately as 10.4 K (Lines[14]) or 14.25 K (Hutchings[16]), either of which is consistent with this overall trend. The core diamagnetism χ_d, computed from $\chi_{Co} = -12 \times 10^{-6}$ emu/mol and the other values given above, is shown in Table II, and agrees closely with $\chi_\perp^0$.

Figure 8 shows $\chi_\parallel$ as a function of $1/T$. Data for pristine $CoCl_2$ obtained by Bizette *et al.*[17] are also shown for comparison. Unlike $\chi_\parallel$ of pristine $CoCl_2$, $\chi_\parallel$ of the intercalation compounds is linear in T^{-1} at large T. Least-squares fits of these data to

$$\chi_\parallel = \chi_\parallel^0 + C_\parallel / T , \tag{23}$$

which is equivalent to Eq. (16) to order T^{-1}, yield $C_\parallel = 2.12$, 2.12, and 2.09 (all emu K/mol); and $\chi_\parallel^0 = 2.8$, 3.8, and 3.5 ($\times 10^{-3}$ emu/mol) for stages 1, 2, and 3, respectively. The parameter $g_\parallel$ obtains as 4.75 (stages 1 and 2) and 4.72 (stage 3). *XY* spin symmetry is confirmed by the fact $g_\perp \gg g_\parallel$.

Once the values of $g_\perp$ and $g_\parallel$ are determined experimentally, ξ can be obtained from Eqs. (13)–(15). Other quantities given parametrically in terms of ξ follow and are shown in Table III. No discernible stage dependence is noted for any of these parameters.

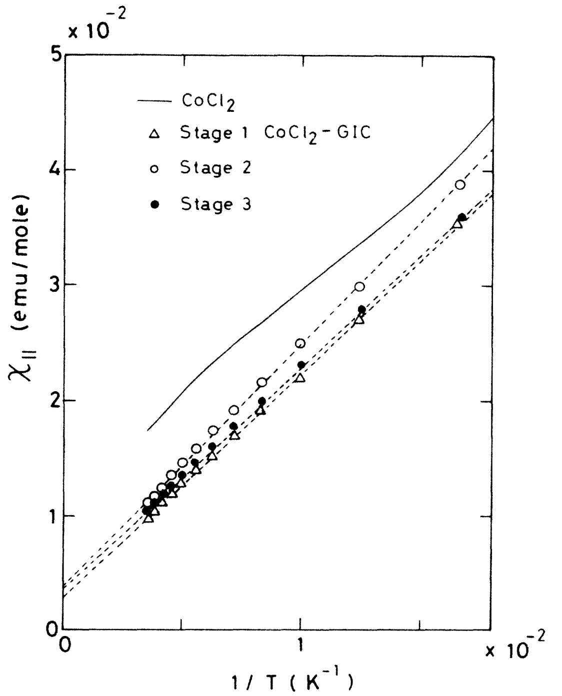

FIG. 8. Susceptibility $\chi_\parallel$ vs $1/T$ for stage-1 -2, and -3 $CoCl_2$-GIC's and for pristine $CoCl_2$ [after Bizette *et al.* (Ref. 17)].

TABLE III. Parameters for stage-1, -2, and -3 $CoCl_2$-GIC's determined from $\chi_\parallel$ data and analysis following Lines (Ref. 14).

	$CoCl_2$-GIC's Stage 1	Stage 2	Stage 3
$g_\parallel$	4.76	4.75	4.72
ξ	2.75	3.15	2.95
δ/λ'	1.42	2.02	1.73
$g_\perp^{(1)}$	4.62	4.75	4.68
$g_\parallel^{(1)}$	3.44	3.10	3.17
Δg	1.33	1.65	1.55
J_A/J	0.38	0.48	0.43
c_1	0.61	0.56	0.58
c_2	−0.68	−0.72	−0.70
c_3	0.41	0.40	0.40

In contrast to $\chi_\perp^0$, which is roughly equal to the core diamagnetism, $\chi_\parallel^0$ is positive and much larger than $|\chi_d|$. The difference can be attributed to Van Vleck paramagnetism. Using the energy levels of the six Kramers doublets obtained from the value of ξ, we calculate the following Van Vleck susceptibilities: $\chi_\parallel^{VV} = 6.9$, 5.5, and 6.3 ($\times 10^{-3}$ emu/mol) for stages 1, 2, and 3, respectively, provided that $\lambda' = -158$ cm^{-1}, as estimated by Lines[14] for $CoCl_2$. These values are in rough agreement with the experimental values of $\chi_\parallel^0$. In sharp contrast, the agreement between $\chi_\perp^{VV}$ and $\chi_\perp^0$ is not good at all, with $\chi_\perp^{VV} \gg |\chi_\perp^0|$.

VI. DISCUSSION

A. $MnCl_2$-GIC

High-temperature susceptibility data show that J is antiferromagnetic and the single-ion anisotropy constant D is positive, indicating *XY* anisotropy. Recent ESR studies[1,2] reveal the two-dimensionality (2D) of these compounds in the $(3\cos^2\theta - 1)^2$ angular dependence of the linewidth. We can conclude that these compounds behave magnetically like 2D *XY*-like antiferromagnets on triangular lattice sites.

Dipole-dipole interactions between spins in the same plane tend to favor the c axis as the easy spin direction, contrary to the observed *XY* spin symmetry. However, an antiferromagnetic coupling between Ising spins on triangular lattice sites leads to a great deal of spin frustration. The observed *XY* behavior therefore means that either the dipole-dipole interaction is small compared to single-ion anisotropy, or that frustration effects raise the ground-state energy enough to make an *XY* configuration energetically favorable.

In 2D *XY* antiferromagnetic systems, the so-called 120° spin structure is expected to occur below the magnetic transition temperature.[18,19] This structure, having a $(\sqrt{3} \times \sqrt{3})$ periodicity, consists of spins on three sublattices forming 120° angles with each other. Recent neutron scattering experiments[5] on the stage-2 compound, however, show that the in-plane structure has a $(2\sqrt{3} \times 2\sqrt{3})$ periodicity incompatible with the 120° structure. This result may be due to the existence of a nonzero interlayer coupling J' or of intraplanar next-nearest-neighbor interactions. As pointed out by Sakakibara[20] for the case of EuC_6, alternatives to the 120° spin structure may arise from a frustration effect of the c-axis stacking sequence of the pristine compound after intercalation. Although the analysis of Sakakibara leads to an incommensurate spin structure, similar considerations may give rise to the $(2\sqrt{3}\times 2\sqrt{3})$ structure observed in $MnCl_2$-GIC.

B. $CoCl_2$-GIC

High-temperature susceptibility data show that J is ferromagnetic and J_A is positive, indicating XY anisotropy. The intraplanar interaction J is found to decrease with increasing stage number. From Eq. (16),

$$\frac{J}{J_0}=(2c_2^2+2\sqrt{3}c_1c_3)^2=\left[\frac{2+24/[\xi(\xi+2)]}{1+6\xi^{-2}+8(\xi+2)^{-2}}\right]^2, \tag{24}$$

where J_0 is a constant relating to the overall average strength of the exchange interactions. Since J/J_0 is a monotonically increasing function of ξ, the decrease of J with stage number suggests the decrease of ξ also. Likewise, J_A/J is a monotonically increasing function of ξ, and this ratio should likewise decrease with increasing stage, making the spin system more isotropic at high stages. Although this interpretation is not supported by the values of ξ obtained from experimental g-values (see Table III), there is some additional evidence for it. In particular, Tsuda *et al.*[21] have recently shown from ^{35}Cl, ^{37}Cl, and ^{59}Co NMR on stage-1 $CoCl_2$-GIC that intercalation into graphite reduces the trigonal deformation of the $CoCl_2$ lattices. It is likely that the decrease of J with stage number results from this reduction of the trigonal deformation.

ACKNOWLEDGMENTS

The authors wish to thank H. Suematsu for providing single crystals of Kish graphite and M. B. Weissman for technical assistance during the susceptibility measurements. This work was supported by NSF under Contract No. DMR 83-04890.

---

*Present address: Department of Physics, State University of New York at Binghamton, Binghamton, NY 13901.

[1] K. Koga and M. Suzuki, J. Phys. Soc. Jpn. **53**, 786 (1984).

[2] O. Gonzalez, S. Flandrois, A. Maaroufi, and J. Amiell, Solid State Commun. **51**, 499 (1984).

[3] Y. Kimishima, A. Furukawa, H. Nagano, P. C. Chow, D. G. Wiesler, H. Zabel, and M. Suzuki, Synth. Metals **12**, 455 (1985).

[4] Y. Kimishima, A. Furukawa, M. Suzuki, and H. Nagano, J. Phys. C **19**, L43 (1986).

[5] M. Suzuki, D. G. Wiesler, P. C. Chow, and H. Zabel, J. Magn. Magn. Mater. **54-57**, 1275 (1986).

[6] Y. Murakami, M. Matsuura, M. Suzuki, and H. Ikeda, J. Magn. Magn. Mater. **31-34**, 1171 (1983).

[7] M. Suzuki, H. Ikeda, and Y. Endoh, Synth. Metals **8**, 43 (1983).

[8] H. Ikeda, Y. Endoh, and S. Mitsuda, J. Phys. Soc. Jpn. **54**, 3232 (1985).

[9] M. Elahy and G. Dresselhaus, Phys. Rev. B **30**, 7225 (1984).

[10] D. G. Wiesler, M. Suzuki, H. Zabel, S. M. Shapiro, and R. M. Nicklow, Physica **136B**, 22 (1986).

[11] D. G. Wiesler, M. Suzuki, and H. Zabel (unpublished).

[12] F. Baron, S. Flandrois, C. Hauw, and J. Gaultier, Solid State Commun. **42**, 759 (1982).

[13] K. Yosida, Prog. Theor. Phys. **6**, 691 (1951).

[14] M. E. Lines, Phys. Rev. **131**, 546 (1963).

[15] A. Abragam and M. H. L. Pryce, Proc. R. Soc. London, Ser. A **206**, 173 (1951).

[16] M. T. Hutchings, J. Phys. C **6**, 3143 (1973).

[17] H. Bizette, C. Terrier, and B. Tsai, C. R. Acad. Sci. **243**, 1295 (1956).

[18] S. Miyashita and H. Shiba, J. Phys. Soc. Jpn. **53**, 1145 (1984).

[19] D. H. Lee, R. G. Caflish, J. D. Joannopoulos, and F. Y. Wu, Phys. Rev. B **29**, 2680 (1984).

[20] T. Sakakibara, J. Phys. Soc. Jpn. **53**, 3607 (1984).

[21] T. Tsuda, H. Yasuoka, and M. Suzuki, Synth. Metals **12**, 461 (1986).